



Evaluating Partial Safety Factors for Shear Strength in Bearing Capacity Calculations for Cohesionless Soils

Amr A. Hemada ¹, Emad A. M. Osman ², Ahmed M. A. Mohamed ^{2*} 

¹ *Geotechnical Engineering Institute, Housing and Building National Research Center, Giza 11511, Egypt.*

² *Department of Civil Engineering, Faculty of Engineering, Minia University, Minya, Egypt.*

Received 13 March 2024; Revised 20 June 2024; Accepted 24 June 2024; Published 01 July 2024

Abstract

Calculating bearing capacity is critical when designing shallow foundations. Many countries use limit state design (LSD) as the standard method for geotechnical design. The paper aims to develop realistic LSD partial factors for bearing capacity calculations of shallow foundations on cohesionless soils based on full-scale model tests. The experimental setup consisted of a hydraulic jack, concrete footing, sand samples, and pressure cells placed in a cylindrical wall. Fifteen sand samples were tested and classified by gradation and relative density. Settlement curves were plotted for each sample under an increasing load. The measured ultimate bearing stresses were found to be higher than theoretical values calculated using traditional methods. This indicates that the traditional approach is conservative. The suggested safety factor for the internal friction angle in cohesionless soils ($\gamma_{\tan(\phi)} = 1.10$) is notably lower than the values specified in Eurocode 7 at 1.25 and the Egyptian code of practice at 1.30. The proposed LSD partial factors allow for more economical designs than traditional factors while maintaining safety. The full-scale model-testing approach is novel and provides realistic factors directly applicable to Egyptian codes. The results are satisfactory and reasonable for the geotechnical design of shallow foundations on cohesionless soils.

Keywords: Full Scale Model; Limit State Design; Working Stress Design; Partial Safety Factor; Calibration.

1. Introduction

The design of any foundation must take into account three key considerations: serviceability limit state (SLS), ultimate limit state (ULS), and engineering economy. The ultimate limit state refers to the point of instability, where the load-carrying capacity reaches its maximum (i.e., the bearing capacity must exceed the applied load), or, in certain situations, the greatest strain or deformation that can be sustained. Whereas, the serviceability limit state requires that the settlement of the designed footing shall not exceed the limits of allowable settlement under normal use [1]. Many design engineers, however, completely disregard the cost side [2].

Geotechnical- strength ULSs are the states associated with or leading to failure or excessive deformations of the ground, such as slope instability and bearing capacity failure. While stability-ULSs include loss of equilibrium of the structure, considered as a rigid body, or loss of equilibrium of the structure or the ground due to uplift by hydrostatic water pressure. The main difference between the aforementioned types of ULSs is that in the first type, the resistance is provided by ground strength, whereas in the later one, the resistance is mainly provided by ground and/or structure weights [3].

* Corresponding author: ahmed.mahdy77@minia.edu.eg

 <http://dx.doi.org/10.28991/CEJ-2024-010-07-015>



© 2024 by the authors. Licensee C.E.J, Tehran, Iran. This article is an open access article distributed under the terms and conditions of the Creative Commons Attribution (CC-BY) license (<http://creativecommons.org/licenses/by/4.0/>).

One of the most important things in geotechnical design is how to define a value for a certain material parameter. Eurocode 7 [4] recommends that this process be done in three steps. The first step is converting test results into derived values (X). The second step is characterization, which entails choosing a suitable characteristic value. The second step is characterization, which involves choosing a suitable characteristic value (X_k) from those derived values; and, finally, a partial factor is applied to the characteristic value to make it more reliable for design purposes (X_d).

The shallow foundation is a component of the substructure that provides support for the superstructure and the loads it carries. The structure comprises the underlying soil and the footings that transmit loads to it [5]. In the process of designing foundations, two parameters are taken into consideration: the ultimate bearing capacity and the limiting settlement. Settlement is a key factor to consider when designing shallow foundations [6, 7]. Assessing the settlement of shallow foundations and calculating their carrying capacity are important and common geotechnical challenges [8]. These problems have been extensively studied as deterministic problems. The significance of the interaction between soil and footing settlement is highlighted in significant scientific publications, which also emphasise its impact on the geometry of the footing [9-18]. Das & Sivakugan [19] argue that when designing shallow foundations with widths more than 1.5 m, it is more crucial to take settlement into account rather than focusing just on bearing capacity. This is especially relevant in engineering practices [20].

The shear strength of the soil is the primary factor that determines the ultimate carrying capacity. This capacity is determined using ideas that have been proposed by Terzaghi [9], Meyerhof [21], Hansen [22], Vesic [23], and other individuals. Foundations are designed to meet both safety requirements to prevent failure and allowable settlement. An evaluation of the safety measures to prevent shear failure caused by compressive pressures must be conducted [20, 24, 25]. A wide range of theoretical, empirical, and computational approaches can be utilised in the process of designing foundations that are subjected to compressive forces or stresses [26, 27]. According to the Egyptian code of practice for soil mechanics, design and construction of foundations number [28], which is drawn from Terzaghi [9], the classic bearing capacity equations (Equation 1) are one of these methodologies.

$$q_{ULS} = C \times N_c \times \lambda_c + \gamma_1 \times D \times N_q \times \lambda_q + \gamma_2 \times N_\gamma \times B \times \lambda_\gamma \quad (1)$$

where C is cohesion of the soil, N_c is bearing capacity factor for the “cohesion” term (dimensionless), λ_c , λ_q and λ_γ are shape factors (dimensionless), γ_1 is unit weight of the overburden material above the base of the footing, D is depth of embedment, N_q is bearing capacity factor for the “surcharge” term (dimensionless), γ_2 is unit weight of the soil under footing, N_γ is bearing capacity factor for the “weight” term (dimensionless), and B is footing width, i.e., least lateral dimension of the footing.

The theories proposed by Terzaghi [9], Meyerhof [21], Hansen [22], and Vesic [23] have provided a means to estimate the bearing capacity of a shallow foundation based on the overall structure of the soil foundation system and probable failure curves. The researchers have conducted multiple studies to examine the accuracy of the theories presented above [29]. Researchers have chosen to focus on either laboratory small scale models or large-scale real footings, depending on their experimental goals. Nevertheless, several researchers contend that small-scale trials lack total reliability due to their observed lack of generalizability. This viewpoint could stem from the presence of uncertainties when applying scaling laws, specifically in scaling up the ratio between the average grain size of soil and the breadth of the foundation (D_{50}/B) [30].

In addition, when it comes to evaluating the bearing capacity of thick sand on cohesionless soils, the various bearing capacity equations exhibit a significant degree of variability [31-34]. Also, the bearing capacities are confirmed by means of laboratory investigations carried out on models manufactured on a smaller scale. Because of the “scale effect” that occurs when large-scale foundations are built on dense sand, shearing strain demonstrates that there is a significant variance along the slip line. Additionally, the average mobilised angle of shearing resistance along the slip line is smaller than the maximum value (Φ_{max}) that is determined by plane shear tests [35]. Because of this, the utilisation of Φ_{max} has the potential to result in an exaggerated bearing capacity value when the calculations are based on various equations [9, 21-23].

Further investigation is required to fully evaluate the actual conduct of small-scale foundations. In the case of real footings on cohesionless, dense soils, the level of shear strain can differ along the slip line. Additionally, the average angle of shear resistance along the slip line may be lower than the highest value (Φ_{max}) that can be achieved from shear tests conducted under plane strain conditions [35]. Therefore, the bearing capacity formula is not conservative and may overestimate the actual bearing capacity of foundations on dense sands. There are also some uncertainties in the requested parameter specifications for measuring the ultimate bearing capacity, such as choosing the best shape factor or depth factor values between those proposed by Terzaghi [9], Meyerhof [21], Hansen [22], and Vesic [23].

In the same regard, Adarsh et al. [36], in their research paper, investigate the use of support vector machines (SVMs) and genetic programming (GP) as soft computing techniques to predict the ultimate bearing capacity of cohesionless soils beneath shallow foundations. Their goal is to investigate how these techniques can accurately determine bearing capacity. The statistical analysis of the results indicates that the implemented models exhibited deficiencies in the theoretical approaches.

Also, Perkins & Madson [37] investigate a new technique for determining the load-bearing capacity of shallow foundations on soils with minimal cohesion, employing a relative density approach. The study utilises full-scale model tests and empirical equations to establish accurate limit state design (LSD) partial factors for bearing capacity estimations. The method under consideration takes into account the relative density of the soil, the constant volume friction angle, and a relative dilatancy index in order to forecast the peak friction angles and ultimate bearing capacities. By integrating progressive failure effects and nonlinear strength behaviour, this methodology provides more accurate predictions compared to conventional methods, hence minimising the requirement for extensive triaxial testing.

This paper's major goal is to calibrate LSD partial safety factors for the shear strength parameters used to calculate bearing capacity for shallow foundations on cohesion less soils. Full scale experimental field-testing program was carried out, to obtain the ultimate bearing capacity of a footing on cohesion less soil and partial safety factors are obtained through back analysis of the obtained test results.

2. Research Methodology

The primary objective of this work is to evaluate partial safety factors for shear strength in bearing capacity calculates for cohesionless soils through the use of full-scale model testing. The following are the primary stages of the methodology (Figure 1):

- Sand samples will be tested in the lab and put into groups by using sieve analysis and direct shear tests to find out their bulk densities and internal friction angles.
- Using a hydraulic jack, a concrete footing, sand samples, and pressure cells to test full-scale models and find out the final bearing stresses and settlements.
- Comparing the measured ultimate bearing stresses to theoretical values computed using conventional methods such as the classical bearing capacity equation.
- Calibrating limit state design (LSD) partial factors for the internal friction angle by back-calculating from the measured ultimate stresses and comparing to allowable bearing capacities using a global factor of safety of 2.5.
- Proposing a lower partial factor for the internal friction angle compared to values specified in Eurocode 7 and the Egyptian code.

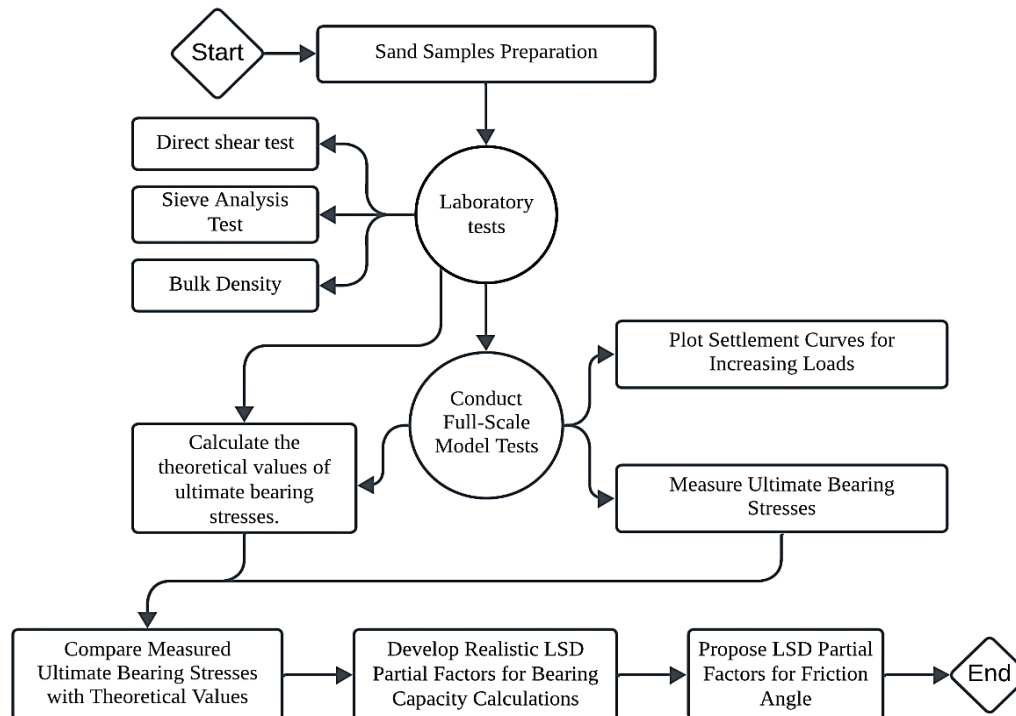


Figure 1. A Typical Flowchart to show the research methodology

3. Results

3.1. Laboratory Results of Tested Sands

Five sand gradations were tested using sieve analysis as plotted in Figure 2. Three different densities of each sand grading (medium dense, dense, and very dense) were investigated.

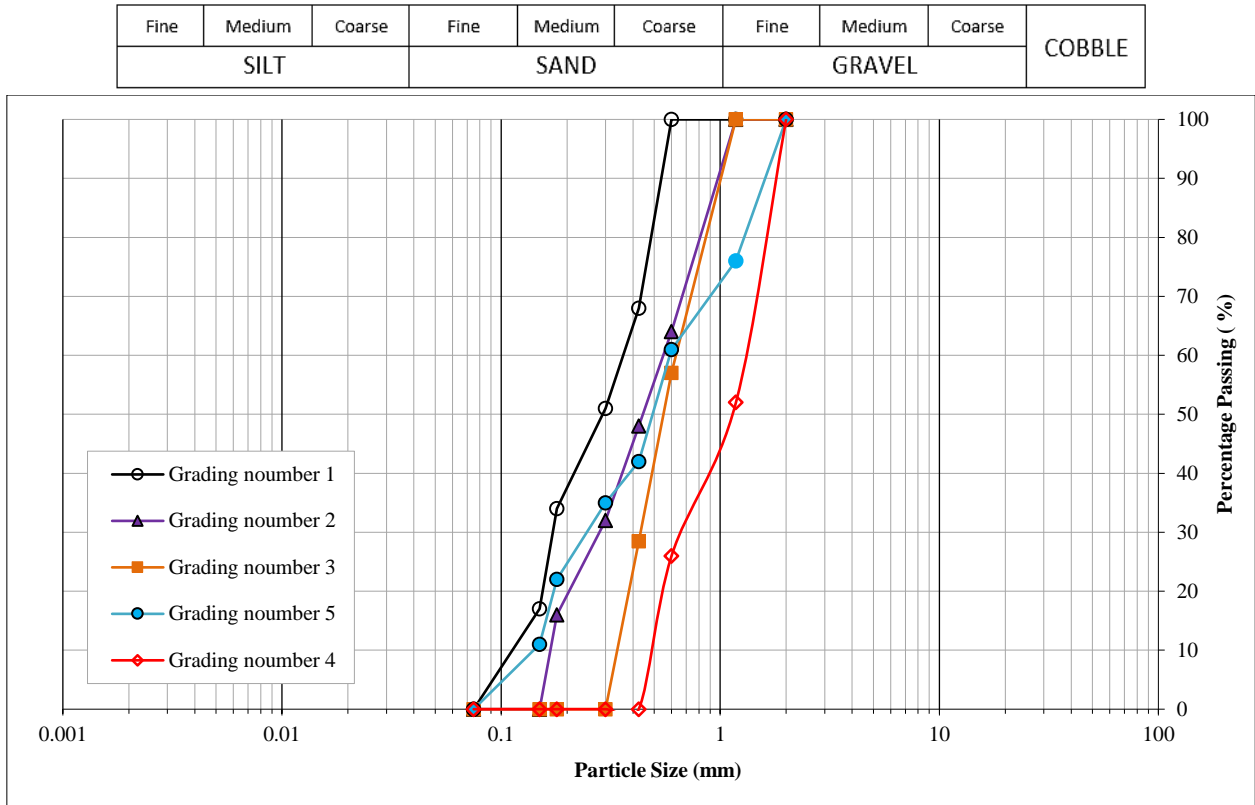


Figure 2. Sieve analysis curves for tested sand samples

The internal friction angles corresponding to each test sample were determined using a direct shear test, and the results are shown in Figure 3. lists the test results. Since density and internal friction angle for sand samples were pre-determined in the laboratory before starting the field tests, it was necessary to reach the same densities specified for each sand sample to ensure achieving the same value of the angle of internal friction for each sample, and this process was controlled by using sand cone tests.

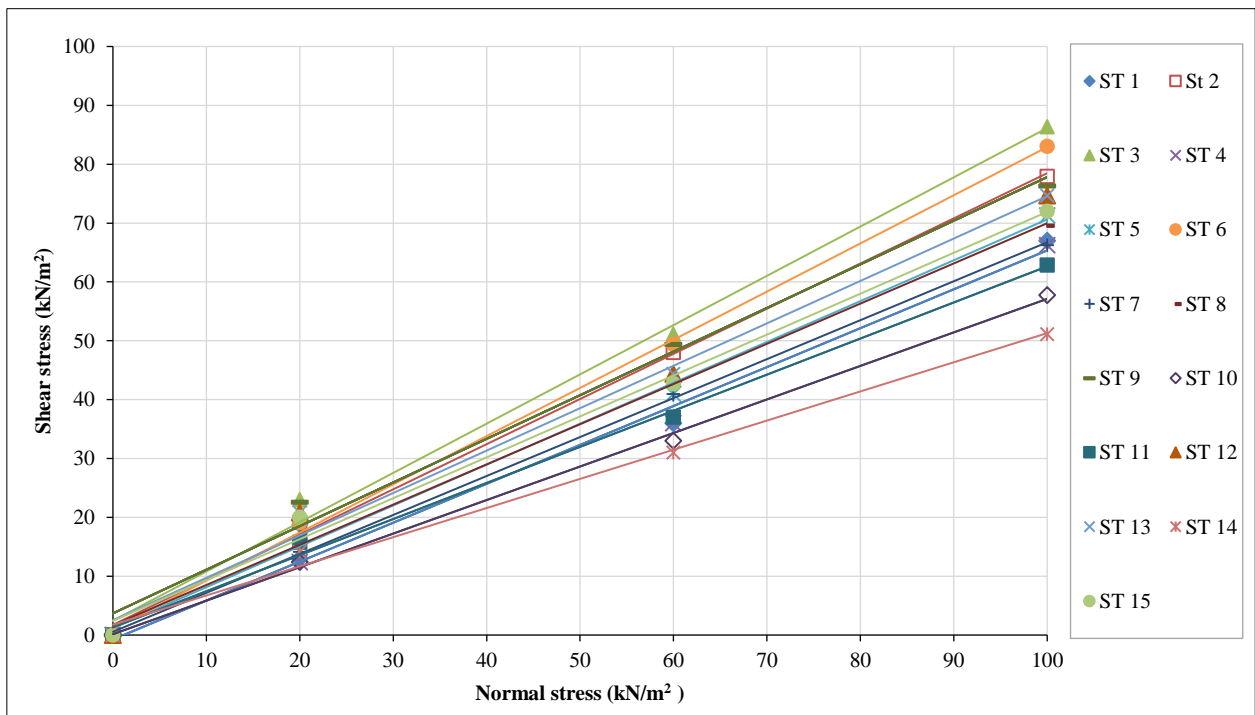


Figure 3. Direct shear test results for tested sand samples

Table 1. Typical results of Internal friction angle (ϕ_k), and bulk density (γ_b)

Sample No.	Samples grades	USCS	ϕ_k °	γ_b (kN/m ³)
ST 1			27.50	15.90
ST 2	Grading No. (1)	Poorly graded sand	32.50	16.10
ST 3			35.00	16.20
ST 4			28.50	16.10
ST 5	Grading No. (2)	Poorly graded sand	33.50	16.70
ST 6			36.00	17.10
ST 7			30.00	15.90
ST 8	Grading No. (3)	Poorly graded sand	34.00	17.10
ST 9			36.50	17.50
ST 10			31.00	15.50
ST 11	Grading No. (4)	Poorly graded sand	36.00	16.50
ST 12			38.00	17.30
ST 13			31.50	16.90
ST 14	Grading No. (5)	Well graded sand	36.50	17.20
ST 15			40.50	17.30

3.2. Field Results of Tested Sands

3.2.1. Field Testing Program

The experimental work is planned to investigate the load settlement behaviour of a model reinforced concrete footing underlain by a sand layer. Fifteen sand types, as described in Table 1, are tested below the model footing using the experimental setup designed especially for the current field-testing program. The full-scale model elements were designed to complete the testing operations without any failure in the system elements.

The experimental setup, designed and used for testing consists of the following main parts as shown in Figure 4:

1. A hydraulic jack equipped with a dial gauge for reading applied loads.
2. A concrete footing 800×800×350 mm, this concrete footing is founded on layers of sand, which are changed every test.
3. An analogue pressure gauge unit connected to a GEKON pressure cell is installed below the foundation for measuring the contact stresses below the footing.
4. Cylindrical-walled tank with a 2800×2250 mm dimension.
5. Two standard IPE 360 mm installed above the upper arm of loading by four steel ties.
6. Two concrete columns are supported by tension piles of 0.40 m in diameter and 10.0 m in depth.
7. Two dial gauges are installed on a reference beam for measuring the footing settlement.



Figure 4. Parts of full-scale model

In each test, after preparing the sand layer, bulk density is measured using the sand cone test to ensure it matches the predefined value. The footing is incrementally loaded using the hydraulic jack up to failure. The pressure cell under the model footing in centric position is used to measure the actual stresses, and the dial gauges are used to determine the footing settlement corresponding to each loading increment.

3.2.2. Stratification of the Natural Soil

To identify the soil characteristics and level of underground water, a geotechnical investigation was carried out, and the soil stratification with respect to the experimental setup is shown in Figure 5.

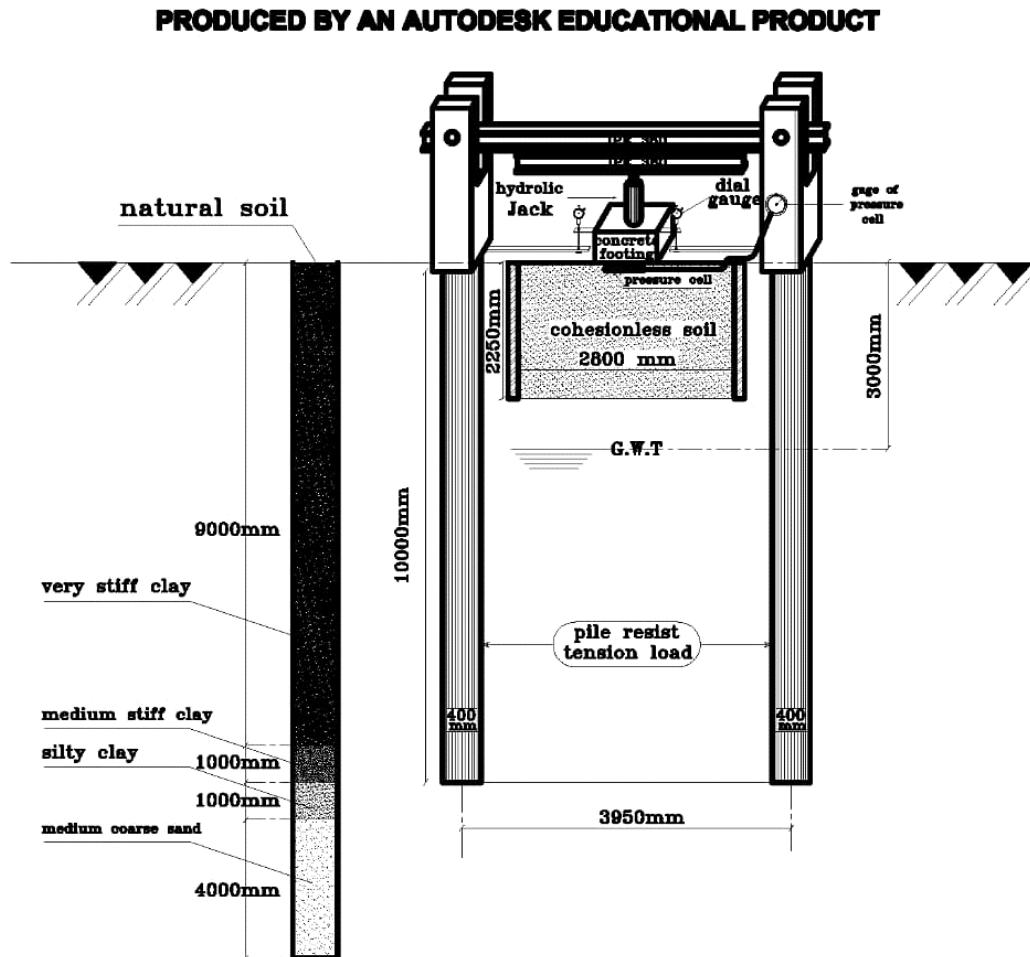


Figure 5. Typical results of boring data for natural soil or subsoil

3.2.3. Measures of Bearing Capacity for Tested Samples

Figure 1 illustrates the division of the sand samples into five groups based on the sieve analysis test. Next, each sample was compacted at three different densities (medium dense, dense, and very dense sand), resulting in a total of 15 samples. Then the angle of internal friction was determined for each of the 15 samples. There were four samples, each of which had the same value for the angle of internal friction (Φ_k). As a result, the total number of samples based on the angle of internal friction was 13. In short, the number of samples according to the sample grading was 5, the number of samples according to the density was 15, and the internal friction angle (Φ_k) was 13 samples.

Fifteen sand samples were tested below the model footing to investigate the load settlement behavior of a model reinforced concrete footing underlain by a sand layer to determine the ultimate stress for each sample. Figure 6 presents the relationship between contact stress and settlement for various soil test samples with medium density and different internal friction angles (Φ_k). The samples with medium density were samples ST 1, ST 4, ST 7, ST 10, and ST 13, as well as samples with low internal friction angle values, ranging from 27.5 for sample ST 1 to 31.5 for sample ST 13. Also, Figure 6 shows that the ultimate stress of the samples increases with an increasing internal friction angle.

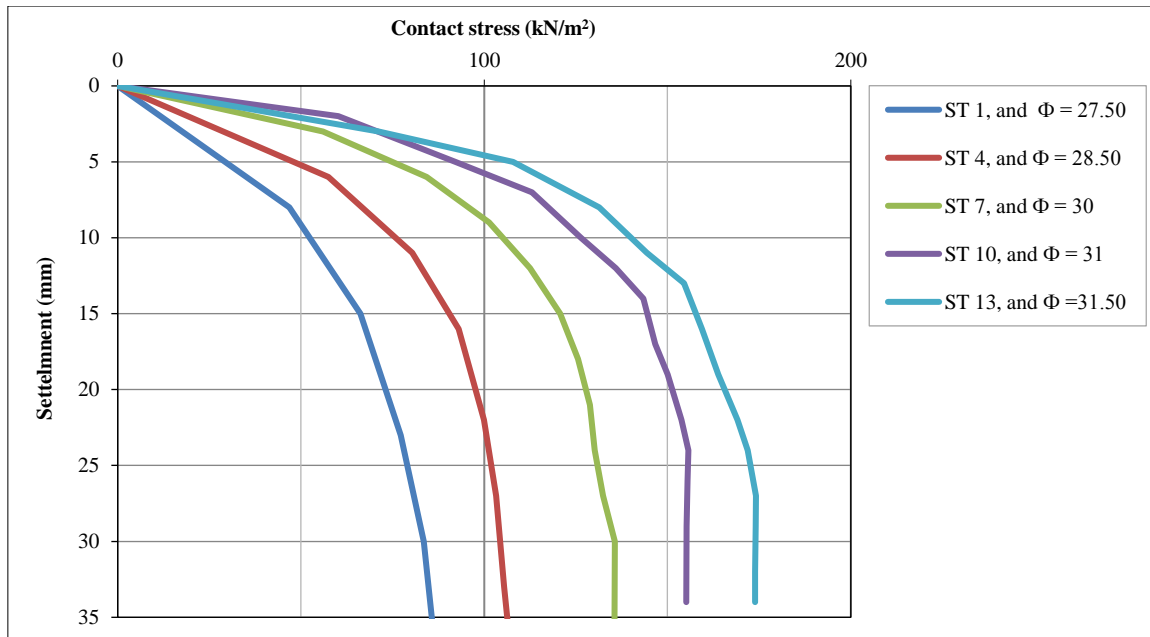


Figure 6. Typical results for stress-settlement curves for medium dense samples

In the same manner, Figure 7 presents the relationship between contact stress and settlement for soil test samples of dense sand with variable internal friction angles (Φ_k). Samples ST 2, ST 5, ST 8, ST 11, and ST 14 were the dense sand group; all of these samples had moderate internal friction angle values, ranging from 32.5 for sample ST 2 to 36.5 for sample ST 14. Also, as the internal friction angle increases, the samples' ultimate stress increases (Figure 7).

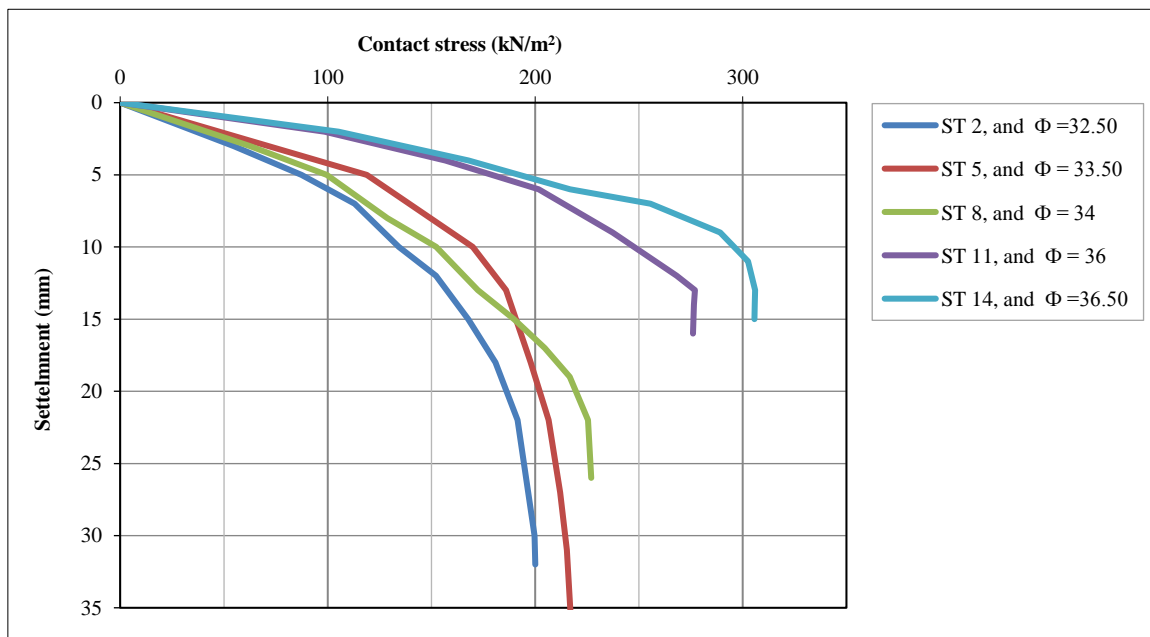


Figure 7. Typical results for stress-settlement curves for dense samples

Similarly, Figure 8 shows the connection between settlement and contact stress for very dense sand soil test samples with varying internal friction angles (Φ_k). Components of the very dense sand group included samples ST 3, ST 6, ST 9, ST 12, and ST 15. All of these samples had high internal friction angle values, with sample ST 3 having the lowest at 35 and sample ST 15 having the highest at 40.5. Figure 8 shows that the samples' final stress increases in relation to the internal friction angle. These curves (Figures 6 to 8) show that the ultimate stress for sand samples typically rises as the sand density and internal friction angle increase.

The results can be arranged according to their classification and values of internal friction angle, as plotted in Figure 9. It is noticed from Figure 9 that samples should be arranged due to their internal angle because the ultimate stress is governed by the value of the internal friction angle and not the sand grading. The ultimate stress for each sample of fifteenth samples was obtained from its load settlement curve (Figures 6 to 8) and listed in Table 2.

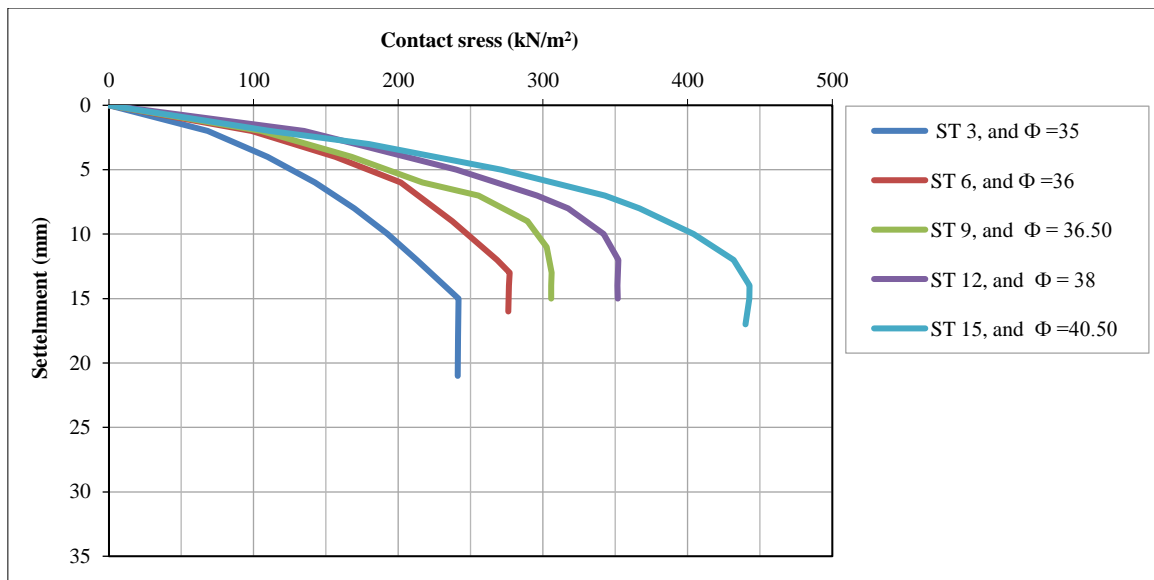


Figure 8. Typical results for stress-settlement curves for very dense samples

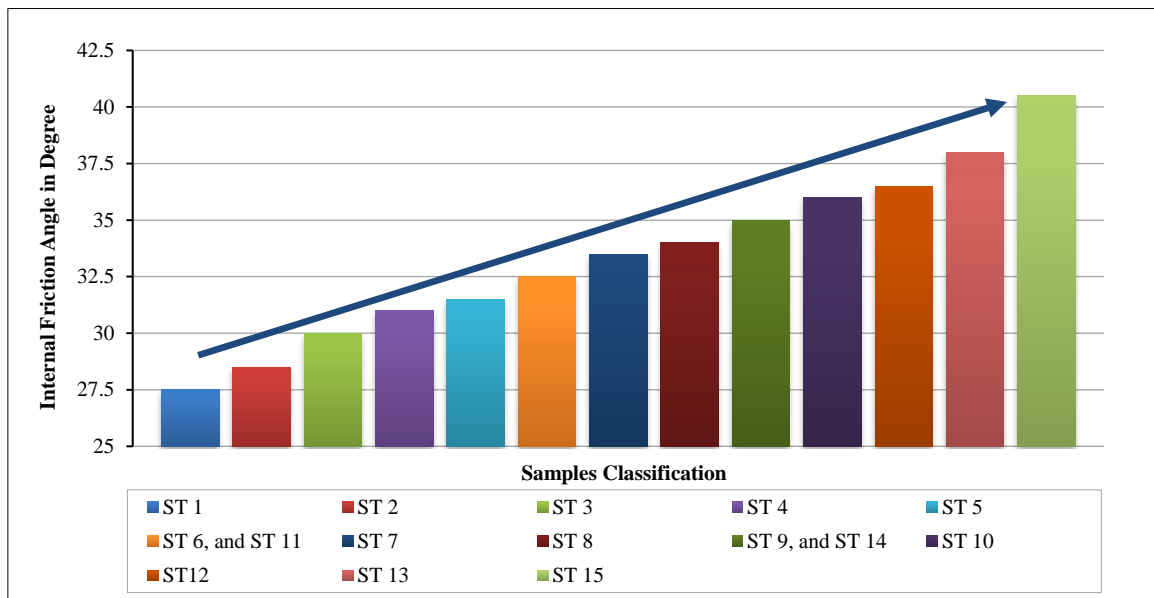


Figure 9. Typical results for arranging samples due to internal friction angle

Table 2. Typical results of ultimate stress

Sample No.	Samples gradations	USCS	Ultimate stress (kN/m ²)
ST 1			90.00
ST 2	Grading No. (1)	SP	200.04
ST 3			241.64
ST 4			108.25
ST 5	Grading No. (2)	SP	219.11
ST 6			276.05
ST 7			135.63
ST 8	Grading No. (3)	SP	227.02
ST 9			305.11
ST 10			155.69
ST 11	Grading No. (4)	SP	276.98
ST 12			352.11
ST 13			174.13
ST 14	Grading No. (5)	SW	305.98
ST 15			442.77

The relationship between internal friction angle (Φ_k), and ultimate measured stress, is plotted in Figure 10. An almost linear relationship between internal friction angle (Φ_k), and ultimate measured stress can be seen in Figure 10.

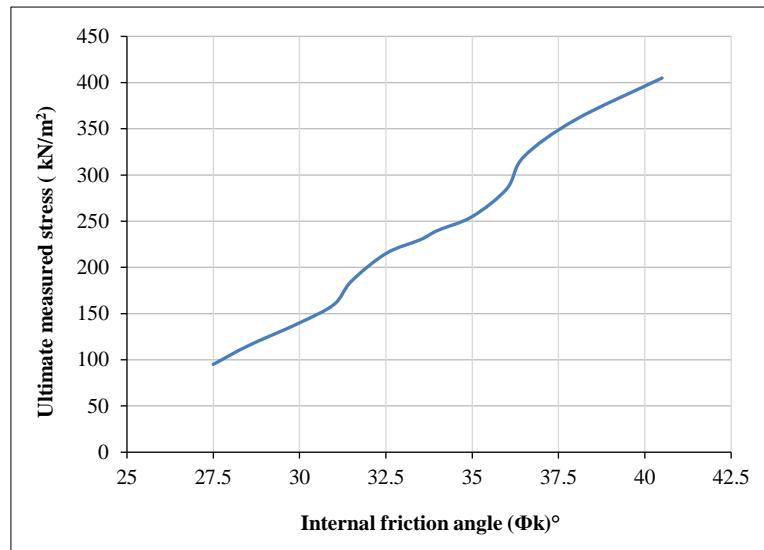


Figure 10. Relationship between internal friction angle (Φ) and ultimate measured stress

3.3. Calibration between Measured and Calculated Ultimate Stress

In this paper, a methodology for calibrating bearing capacity partial factors is presented, making use of the measured ultimate stress obtained from field testing of the full-scale model. The calibration methodology involves several steps:

- Evaluation of ultimate bearing capacity values based on the classical bearing capacity equation for every value of internal angle.
- Calculate the allowable bearing capacity based on a global factor of safety of 2.5.
- Back calculation of LSD partial factors ($\gamma_{\tan \phi}$) from the measured ultimate stress that yields the same footing dimensions as obtained from the allowable bearing capacity (WSD) for every value of internal friction angle.
- The above procedures assume that the critical combination for the design of footing dimensions is that it considers characteristic values for the load and factored shear strength parameters, which compares to approach 1 and combination 2 of EC7.

3.3.1. Calculate Ultimate and Allowable Bearing Capacity Using the Traditional Method

The classical bearing capacity equation (ECP 202/3 (2001)) is used for the calculation of the ultimate stress for each sample (Equation 2). The bearing capacity equation for the tested case of footing on a ground surface may be reduced to the following form:

$$q_{ult(calculated)} = \gamma B N_{\gamma} \lambda_{\gamma} \quad (2)$$

where γ is dry density, $B = 0.80$ m, $N_q = e^{\pi \tan \phi} \cdot \tan^2(45 + \frac{\phi}{2})$, $N_{\gamma} = (N_q - 1) \tan \phi$, and $\lambda_{\gamma} = 1 - 0.3 \left(\frac{B}{L}\right) = 1 - 0.3 = 0.70$

The calculated bearing capacity for all samples is listed in Table 3. It can be seen from this table that the calculated values of bearing capacity are considerably lower than their corresponding measured values, which means that the theoretical calculations of bearing capacity for the studied cases are conservative.

3.3.2. Determination of LSD Partial Factors

The determination of the LSD partial factor, which achieves bearing capacity values equal to those obtained via WSD and measured ultimate stress, can be accomplished using a statistical method utilizing trial and error. This can be done by utilizing an Excel sheet to record and analyze the findings. Table 4 presents the obtained partial safety factor corresponding to each studied case making use of the methodology outlined earlier in this section. It can be seen from this table that the calibrated partial factor of safety ($\gamma_{\tan \phi}$) ranges between 1.03 to 1.08. A factor of safety of 1.10 satisfies all the studied cases. For comparison purpose, the partial safety factor ($\gamma_{\tan \phi}$) values in EC7 and the ECP are 1.25 and 1.30 respectively. It can be seen that both codes provide a conservative estimate of the partial factor of safety compared to that obtained from the back analysis of the measured cases.

Table 3. Calculated the ultimate and allowable bearing capacity value

ϕ_k	γ (kN/m ³)	N_γ	$q_{ult}(\text{calculated})$ (kN/m ²)	$q_{all}(\text{calculated})$ (kN/m ²)
27.5	15.90	6.73	59.96	23.98
28.5	16.10	7.90	71.25	28.50
30	15.90	10.05	89.45	35.78
31	15.50	11.80	102.38	40.95
31.5	16.90	12.78	120.99	48.39
32.5	16.10	15.02	135.47	54.19
33.5	16.70	17.68	165.32	66.13
34	17.10	19.18	183.70	73.48
35	16.20	22.61	205.15	82.06
36	16.50	26.70	246.73	98.69
36.5	17.20	29.04	279.67	111.87
38	17.30	37.45	362.81	145.12
40.5	17.50	57.95	567.86	227.15

Table 4. Calibrated partial safety factors for shear strength obtained for tested samples

Characteristic internal friction angle (ϕ_k)°	Allowable Bearing (WSD) (kN/ m ²)	Measured ultimate stress. stress (kN/ m ²)	Partial safety factor corresponding to measured ultimate stress. ($\gamma_{\tan \phi}$)
27.5	23.98	90.00	1.03
28.5	28.50	108.25	1.03
30	35.78	135.63	1.03
31	40.95	155.69	1.03
31.5	48.39	174.13	1.03
32.5	54.19	200.04	1.03
33.5	66.13	219.11	1.03
34	73.48	227.02	1.08
35	82.06	241.64	1.08
36	98.69	276.98	1.08
36.5	111.87	305.98	1.08
38	145.12	352.11	1.08
40.5	227.15	442.77	1.08

4. Conclusions

The geotechnical limit state design method proved to be the most efficient method for the design of foundations. It satisfies both safety and economic requirements. The most important conclusions obtained based on the field testing carried out on a full-scale model footing resting on sandy soils are as follows:

- For the five investigated gradings of sand, it was found that the coarse gradings of the sand yield a higher internal friction angle for the same density and thus higher ultimate stresses.
- Each sand grade was compacted into three densities, which are medium dense sand, dense sand, and very dense sand. It was found that the measured ultimate stress is directly proportional to sand density.
- Compared with the results of the field testing, the classical bearing capacity equation of Terzaghi gives a conservative estimate of the bearing capacity for shallow foundations on cohesion-less soils.
- The calibration methodology proposed in this paper resulted in a partial safety factor for internal friction angle for cohesion-less soils ($\gamma_{\tan(\phi)} = 1.10$). The proposed factor gives a reliable and economical design for sandy soils when calculating ultimate bearing capacity using Terzaghi's equation.
- The proposed safety factor for internal friction angle for cohesion-less soils ($\gamma_{\tan(\phi)} = 1.10$) is considerably lower than the value used in EC7 (DA1-b), which is 1.25, as well as the value used in the Egyptian code of practice, which is (1.30).

5. Declarations

5.1. Author Contributions

Conceptualization, A.A.H. and E.A.M.O.; methodology, A.M.A.M.; software, A.M.A.M.; validation, A.M.A.M.; investigation, A.A.H., E.A.M.O, and A.M.A.M.; writing—original draft preparation, A.M.A.M.; writing—review and editing, A.A.H., E.A.M.O., and A.M.A.M.; visualization, A.M.A.M.; supervision, A.A.H. and E.A.M.O. All authors have read and agreed to the published version of the manuscript.

5.2. Data Availability Statement

The data presented in this study are available on request from the corresponding author.

5.3. Funding

The authors received no financial support for the research, authorship, and/or publication of this article.

5.4. Conflicts of Interest

The authors declare no conflict of interest.

6. References

- [1] Móczár, B., & Szendefy, J. (2017). Calculation of presumed bearing capacity of shallow foundations according to the principles of eurocode 7. *Periodica Polytechnica Civil Engineering*, 61(3), 505–515. doi:10.3311/PPci.8553.
- [2] Söderholm, P. (2020). The green economy transition: the challenges of technological change for sustainability. *Sustainable Earth*, 3(1), 6. doi:10.1186/s42055-020-00029-y.
- [3] Abdel-Fattah, T. (2017). Employment of reliability analysis to assess soil strength partial factors for slope stability problems. *International Conference on Advances in Structural and Geotechnical Engineering, ICASGE, 27-30 March, 2017, Hurghada, Egypt*.
- [4] EN 1997-1:2004. (2004). *Eurocode 7: Part 1, General Rules*. European Committee for Standardization, Brussels, Belgium.
- [5] Pujadas-Gispert, E., Sanjuan-Delmás, D., & Josa, A. (2018). Environmental analysis of building shallow foundations: The influence of prefabrication, typology, and structural design codes. *Journal of Cleaner Production*, 186, 407–417. doi:10.1016/j.jclepro.2018.03.105.
- [6] Kim, Y., Park, H., & Jeong, S. (2017). Settlement behavior of shallow foundations in unsaturated soils under rainfall. *Sustainability (Switzerland)*, 9(8), 1417. doi:10.3390/su9081417.
- [7] Johnson, K., Christensen, M., Sivakugan, N., & Karunasena, W. (2003). Simulating the response of shallow foundations using finite element modelling. *Proceedings of the MODSIM 2003 International Congress on Modelling and Simulation, 14-17 July, 2003, Townsville, Australia*.
- [8] Enkhtur, O., Nguyen, T. D., Kim, J. M., & Kim, S. R. (2013). Evaluation of the settlement influence factors of shallow foundation by numerical analyses. *KSCE Journal of Civil Engineering*, 17, 85-95. doi:10.1007/s12205-013-1487-2.
- [9] Terzaghi, K. (1943). *Theoretical Soil Mechanics*. Wiley, New York, United States. doi:10.1002/9780470172766.
- [10] Michalowski, R. L. (1997). An estimate of the influence of soil weight on bearing capacity using limit analysis. *Soils and Foundations*, 37(4), 57–64. doi:10.3208/sandf.37.4_57.
- [11] Michalowski, R. L. (2001). Upper-bound load estimates on square and rectangular footings. *Geotechnique*, 51(9), 787–798. doi:10.1680/geot.2001.51.9.787.
- [12] Martin, C. M. (2005). Exact bearing capacity calculations using the method of characteristics. *Torino International conference of International Association for Computer Methods and Advances in Geomechanics (IACMAG), 19-24 June, 2005, Torino, Italy*.
- [13] Zafeirakos, A., & Gerolymos, N. (2016). Bearing strength surface for bridge caisson foundations in frictional soil under combined loading. *Acta Geotechnica*, 11(5), 1189–1208. doi:10.1007/s11440-015-0431-7.
- [14] Zhou, H., Zheng, G., Yin, X., Jia, R., & Yang, X. (2018). The bearing capacity and failure mechanism of a vertically loaded strip footing placed on the top of slopes. *Computers and Geotechnics*, 94, 12–21. doi:10.1016/j.compgeo.2017.08.009.
- [15] Sultana, P., & Dey, A. K. (2019). Estimation of Ultimate Bearing Capacity of Footings on Soft Clay from Plate Load Test Data Considering Variability. *Indian Geotechnical Journal*, 49(2), 170–183. doi:10.1007/s40098-018-0311-9.
- [16] Papadopoulou, K., & Gazetas, G. (2020). Shape Effects on Bearing Capacity of Footings on Two-Layered Clay. *Geotechnical and Geological Engineering*, 38(2), 1347–1370. doi:10.1007/s10706-019-01095-6.

- [17] Fu, D., Zhang, Y., & Yan, Y. (2020). Bearing capacity of a side-rounded suction caisson foundation under general loading in clay. *Computers and Geotechnics*, 123, 103543. doi:10.1016/j.compgeo.2020.103543.
- [18] Li, S., Yu, J., Huang, M., & Leung, C. F. (2021). Upper bound analysis of rectangular surface footings on clay with linearly increasing strength. *Computers and Geotechnics*, 129, 103896. doi:10.1016/j.compgeo.2020.103896.
- [19] Das, B. M., & Sivakugan, N. (2007). Settlements of shallow foundations on granular soil - An overview. *International Journal of Geotechnical Engineering*, 1(1), 19–29. doi:10.3328/IJGE.2007.01.01.19-29.
- [20] Hakro, M. R., Kumar, A., Ali, M., Habib, A. F., de Azevedo, A. R. G., Fediuk, R., Sabri, M. M. S., Salmi, A., & Awad, Y. A. (2022). Numerical Analysis of Shallow Foundations with Varying Loading and Soil Conditions. *Buildings*, 12(5), 693. doi:10.3390/buildings12050693.
- [21] Meyerhof, G. G. (1963). Some Recent Research on the Bearing Capacity of Foundations. *Canadian Geotechnical Journal*, 1(1), 16–26. doi:10.1139/t63-003.
- [22] Hansen, J.B. (1961) A General Formula for Bearing Capacity. Bulletin No. 11, Danish Geotechnical Institute, Copenhagen, Denmark.
- [23] Vesić, A. S. (1973). Analysis of Ultimate Loads of Shallow Foundations. *Journal of the Soil Mechanics and Foundations Division*, 99(1), 45–73. doi:10.1061/jsfeaq.0001846.
- [24] Schneider-Muntau, B., & Bathaeian, I. (2018). Simulation of settlement and bearing capacity of shallow foundations with soft particle code (SPARC) and FE. *GEM - International Journal on Geomathematics*, 9(2), 359–375. doi:10.1007/s13137-018-0109-z.
- [25] Esmaeili, K., Eslami, A., & Rezazadeh, S. (2018). Semi-Deep Skirted Foundations and Numerical Solution to Evaluate Bearing Capacity. *Open Journal of Geology*, 08(06), 623–640. doi:10.4236/ojg.2018.86036.
- [26] Chua, B. T., Abuel-Naga, H., & Nepal, K. P. (2023). Design Charts for Geogrid-Reinforced Granular Working Platform for Heavy Tracked Plants over Clay Subgrade. *Transportation Infrastructure Geotechnology*, 10(5), 795–815. doi:10.1007/s40515-022-00243-5.
- [27] Shahnazari, H., & Tutunchian, M. A. (2012). Prediction of ultimate bearing capacity of shallow foundations on cohesionless soils: An evolutionary approach. *KSCE Journal of Civil Engineering*, 16(6), 950–957. doi:10.1007/s12205-012-1651-0.
- [28] ECP 202/1. (2005). Egyptian code for soil mechanics – design and construction of foundations. Part 1, Site investigation. The Housing and Building Research Center (HBRC), Cairo, Egypt.
- [29] Hjjaj, M., Lyamin, A. V., & Sloan, S. W. (2005). Numerical limit analysis solutions for the bearing capacity factor N_γ . *International Journal of Solids and Structures*, 42(5–6), 1681–1704. doi:10.1016/j.ijsolstr.2004.08.002.
- [30] Steenfelt, J. S. (1977). Scale Effect on Bearing Capacity Factor N_γ . The 9th International Conference on Soil Mechanics and Foundation Engineering ICSMFE, Tokyo, Japan.
- [31] Cassidy, M. J., & Houslyby, G. T. (2002). Vertical bearing capacity factors for conical footings on sand. *Geotechnique*, 52(9), 687–692. doi:10.1680/geot.2002.52.9.687.
- [32] Krabbenhoft, S., Damkilde, L., & Krabbenhoft, K. (2014). Bearing Capacity of Strip Footings in Cohesionless Soil Subject to Eccentric and Inclined Loads. *International Journal of Geomechanics*, 14(3), 4014003. doi:10.1061/(asce)gm.1943-5622.0000332.
- [33] Valore, C., Ziccarelli, M., & Muscolino, S. R. (2017). The bearing capacity of footings on sand with a weak layer. *Geotechnical Research*, 4(1), 12–29. doi:10.1680/jgere.16.00020.
- [34] Mansour, M. F., Saad El-Din, M. D., El-Mossallamy, Y. M., & Mahdi, H. A. (2018). Application of the ultimate limit states factored strength approach to design of cantilever walls in dry cohesionless soils. *HBRC Journal*, 14(3), 415–421. doi:10.1016/j.hbrj.2018.02.001.
- [35] Padmini, D., Ilamparuthi, K., & Sudheer, K. P. (2008). Ultimate bearing capacity prediction of shallow foundations on cohesionless soils using neurofuzzy models. *Computers and Geotechnics*, 35(1), 33–46. doi:10.1016/j.compgeo.2007.03.001.
- [36] Adarsh, S., Dhanya, R., Krishna, G., Merlin, R., & Tina, J. (2012). Prediction of Ultimate Bearing Capacity of Cohesionless Soils Using Soft Computing Techniques. *ISRN Artificial Intelligence*, 2012, 1–10. doi:10.5402/2012/628496.
- [37] Perkins, S. W., & Madson, C. R. (2000). Bearing Capacity of Shallow Foundations on Sand: A Relative Density Approach. *Journal of Geotechnical and Geoenvironmental Engineering*, 126(6), 521–530. doi:10.1061/(asce)1090-0241(2000)126:6(521).